EFFECT OF VIBRATIONS ON THE DYNAMICS OF THE RING RESONATOR MICROMECHANICAL GYROSCOPE

The Trung Giap Vu[1,*]

[1]*Faculty of Aerospace Engineering, Le Quy Don Technical University*

Abstract

This article examines the dynamics of a micromechanical gyroscope with a ring resonator, used in navigation and motion control systems. The gyroscope's sensitive element consists of a thin elastic ring resonator supported by an elastic suspension, detecting small bending vibrations to measure angular motion. The study investigates the impact of external vibrations on the resonator's mechanical design. A mathematical model is developed using the Hamilton-Ostrogradsky variational principle and the Bubnov-Galerkin projection method to analyze the system's multimodal oscillations. Results show that vibrations mainly affect the first vibrational mode, with maximum deformation of the resonator is proportional to the magnitude of the peak impact acceleration and inversely proportional to the square of the lowest natural frequency in the first natural mode of oscillation. The second vibrational mode remains unaffected under normal conditions. Additionally, manufacturing errors can cause symmetry violations, impacting measurement accuracy. This study provides insights into improving ring resonator micromechanical gyroscope design for enhanced reliability under dynamic external vibrations.

Keywords: *Micromechanical gyroscope; ring resonator; nonlinear dynamics.*

1. Introduction

This research focuses on the micromechanical gyroscope with a ring resonator (RMMG), a crucial component in modern navigation and motion control systems. The RMMG's sensitive element is modeled as an elastic ring resonator supported by an elastic suspension. Its function relies on measuring minute bending vibrations of the ring resonator, which in turn determines the angular motion of the gyroscope's base around its sensitivity axis, perpendicular to the ring's plane. The primary objective of this study is to investigate the RMMG's dynamics under vibration conditions to assess the reliability of its mechanical design.

The reliability of mechanical systems is influenced by a combination of factors: random external loads, the intrinsic properties of the system and its components, the nature of element interactions, and specific design and technological features [1], [2].

[*] Corresponding author, email: vuthetrunggiap@lqdtu.edu.vn
DOI: 10.56651/lqdtu.jst.v21.n1.1072

Previous foundational research [3]-[5] has established fundamental models and analyses of gyroscopic physical processes and imperfections that contribute to drift, providing a crucial basis for accurate mathematical modeling. Specifically, the impact of vibrations on the resonant wave pattern of ring resonators has been addressed [6], which is critical for understanding micromechanical gyroscope behavior under dynamic loads. Comprehensive studies on the dynamics of micromechanical and solid-state gyroscopes support multimode dynamic modeling [7], while asymptotic methods and computational mechanics tools [8], [9] aid in effective simulation and analytical solutions for flexible structures like RMMG resonators. Furthermore, research on the design and vibration sensitivity of MEMS ring gyroscopes [10]-[12] offers important insights into structural and functional optimization.

Recent advancements, particularly in studies by Maslov *et al.* [13]-[17], have extensively explored nonlinear effects in electrostatic control systems and proposed methods to mitigate them. These findings are vital for enhancing micromechanical gyroscope accuracy and stability when subjected to external disturbances. Expanding on this, other works [18]-[20] delve into real-time correction methods and advanced modeling of microshell and flat-electrode resonator gyroscopes. The examination of nonlinear vibration phenomena using uncertainty analysis [21] and the study of critical parameters influencing micromechanical gyroscope behavior under electrostatic forces [22] further contribute to a deeper understanding of RMMG dynamics. Finally, the practical integration of advanced gyroscopic models into navigation systems [23] underscores the paramount importance of reliability and dynamic precision in real-world applications.

Recent research has increasingly focused on nonlinear resonance and stability phenomena in vibrating and gyroscopic systems. Amer *et al.* [24] investigated the stability of autoparametric dynamical systems in the vicinity of resonance, revealing bifurcation behaviors that are particularly relevant to MEMS resonators. Bek *et al.* [25] extended this line of inquiry by conducting an asymptotic analysis of three-degree-of-freedom systems near resonance, providing analytical tools for a deeper understanding of coupled oscillations in micromechanical gyroscopes. Furthermore, Amer [26] explored the rotational dynamics of gyrostats with asymmetric mass distribution, demonstrating how structural imbalance can introduce nonlinear perturbations. More recently, Amer and co-authors [27], [28] examined the combined influence of external torques, gyrostatic moments, and energy dissipation on the stability of rigid bodies and spacecraft, drawing

important parallels with control challenges in MEMS gyroscopes. Complementing these studies, their investigations of Euler's equations with time-dependent gyrostatic torques [29] and the modeling of Euler-Poisson equations under gyrostatic effects [30] introduced innovative methodologies for analyzing nonlinear gyroscopic dynamics.

Assessing the reliability of such a mechanical system typically involves several key stages. Initially, the mechanical system's design scheme is chosen, and a mathematical model is constructed, accounting for its operational characteristics. Given that the RMMG is a system with distributed parameters, the Hamilton-Ostrogradsky variational principle and the Bubnov-Galerkin projection method are employed to formulate a mathematical model describing the motion of the micromechanical gyroscope resonator. The resulting differential equations, which describe the oscillations of the elastic system in a multimode approximation, are then analyzed using asymptotic methods of mechanics [31] and statistical dynamics [32]-[35]. The ultimate goal of this problem-solving process is to determine the maximum deformations and stresses within the RMMG, which serve as the basis for evaluating the reliability of its mechanical structure. This study specifically aims to develop a mathematical model of the micromechanical gyroscope resonator to analyze its dynamic behavior under vibration and subsequently assess the system's structural reliability based on calculated stress and deformation responses.

2. Dynamics of the ring resonator micromechanical gyroscope

2.1. Mathematical model of the ring resonator

The RMMG is a thin elastic ring 2 connected to the base 1 by lamellas 3 which are elastic suspension elements (Fig. 1). The thickness of the resonator h, and the axial line in the undeformed state is a circle with a radius R. Resonator 1 is manufactured by plasma-chemical etching together with elastic suspension elements. The oscillations of the resonator are excited and recorded by a system of control and measuring circuits. Each circuit is formed by two nearest lamellas and a resonator section with circumferential size $\pi / 4$.

The right Cartesian coordinate system $Ox_1x_2x_3$ is defined with respect to the base of the gyroscope, with the Ox_1x_2 plane containing the elastic ring. To describe the deformations of the resonator, the orthogonal coordinate system $y_1y_2y_3$ is introduced, in which the elastic displacement vector of the ring resonator element is defined as $\mathbf{u} = v, w, 0^{T}$, where $v = v(t, \varphi)$ and $w = w(t, \varphi)$ represent deformations in the circumferential and radial directions, respectively, as functions of time t and angular coordinate φ.

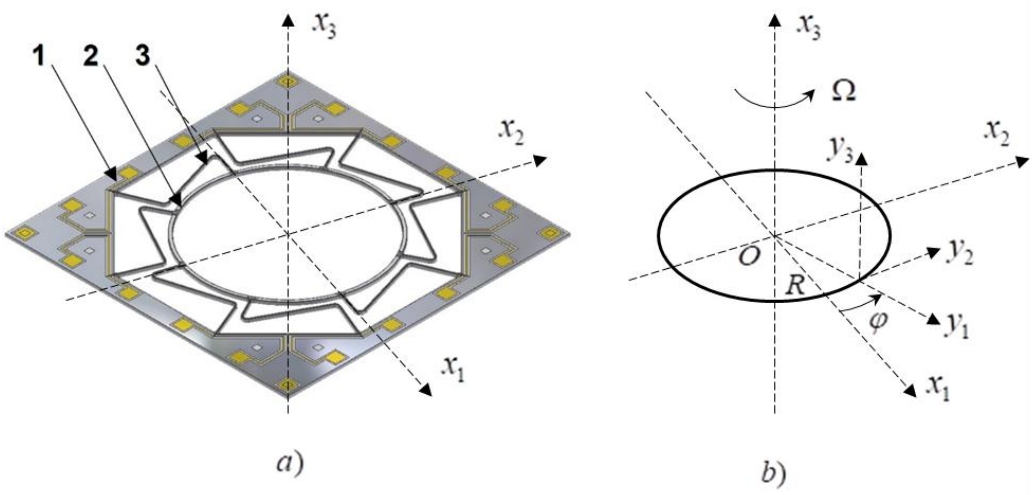

Fig. 1. Ring resonator micromechanical gyroscope (a) and coordinate systems (b).

Assuming that the resonator mounting axis rotates around the axis with a slowly varying angular velocity $\Omega(t)$, which is considered small in comparison to the main resonator oscillation frequency ω. To obtain a mathematical model of a ring resonator in an elastic suspension, the Winkler foundation model [7], [9] is employed. To account for the influence of base vibrations, the masses of eight supporting lamellas in the elastic suspension connected to the elastic ring are additionally considered.

Considering the motion of the resonator in the plane Ox_1x_2, the absolute velocities of point O projected onto the x_1, x_2 axes are defined as $V_1(t), V_2(t)$, respectively. In this case, the specific kinetic energy of the thin elastic ring, referred to the unit length of the resonator axial line, is expressed in Eq. (1) as:

$$T = \frac{\rho RS\left(1+\mu_*(\varphi)\right)}{2}\Big[\left(\dot{v}+\Omega\left(w+R\right)-V_1\sin\varphi+V_2\cos\varphi\right)^2 + \\ +\left(\dot{w}-\Omega v+V_1\cos\varphi+V_2\sin\varphi\right)^2\Big], \tag{1}$$

where ρ, R are the material density and resonator radius, respectively; $S = bh$ is the cross-sectional area of the resonator, h is the thickness of the resonator, b is the height of the cross-section and suspension torsion bars; μ_* is the relative attached mass of the elastic suspension of the resonator, presented as an expansion in a Fourier series along the circumferential coordinate φ:

$$\mu_*(\varphi) = \mu_0 + \sum_{k=1}^{N}\left(\mu_k\cos k\varphi + \bar{\mu}_k\sin k\varphi\right),$$

where $\mu_k, \bar{\mu}_k$ are the expansion coefficients. In the case of an ideally manufactured symmetric elastic system, the coefficients with numbers 1, 2,..., 7 are equal to zero. In Eq. (1) and below, the dot denotes the time derivative *t*.

The elastic properties of a single-crystal resonator obey the generalized Hooke's law [35]. The technique to calculate the elastic properties of the resonator material and obtaining differential equations of motion of an elastic system is described in [7].

Taking into account the uniaxial stress state of the ring resonator, the relationship between the stress σ and the hoop deformation e is expressed as follows:

$$\sigma = E\, e, \tag{2}$$

where E is Young's modulus, which generally depends on the direction cosines of the direction of the axis y_2 (Fig. 1) in the principal axes of the crystal. According to the technology, the resonator is made from a single-crystal silicon wafer L-cut, i.e. in the plane, while the Young's modulus in the plane of the crystal does not depend on the direction of the axis y_2.

Note that due to instrumental errors in the manufacture of the resonator, the orientation of the single-crystal plate may differ from the calculated one, which will lead to a small change in the Young's modulus with a change in the circumferential coordinate φ along the direction y_2. The magnitude of the splitting frequency of the resonator oscillations, caused by instrumental manufacturing errors, as a rule, does not exceed 1-3 Hz, which is significantly by four orders of magnitude less than the main natural frequency of the resonator oscillations.

To study the reliability of the mechanical structure, the reliability indicator is calculated based on the maximum stress value in the cross section of the ring resonator and the elastic suspension lamellas. The condition of failure-free operation of the resonator will be characterized by the absence of plastic deformations of the structural elements. The strain energy per unit volume of the resonator, taking into account, the Eq. (2) has the form [7]:

$$P = \int_0^e \sigma\, de = \frac{1}{2} E e^2 \tag{3}$$

The expression for the circumferential deformation is determined by the relation [7]:

$$e = \frac{1}{R}\left(v' + w\right) - \frac{\varsigma}{R^2}\left(v' - w''\right), \tag{4}$$

where ς is the coordinate measured from the median line of the resonator in the direction of the outer normal $\left(-h/2 \le \varsigma \le h/2\right)$. In Eq. (4) and below, the prime denotes the partial derivative with respect to the circumferential coordinate φ.

After substitution and integration over the cross-sectional area of the resonator S, the specific potential energy is obtained:

$$P = \frac{1}{2}\left[\frac{E\,S}{R}\left(v' + w\right)^2 + \frac{E\,I}{R^3}\left(v' - w''\right)^2\right] + \frac{1}{2}c(\varphi)\left(v^2 + w^2\right) + q(t,\varphi)Rw\,, \tag{5}$$

where I is the moment of inertia of the resonator cross section (for a rectangular cross section $I = bh^3/12$), $q\left(t,\varphi\right)$ is the specific strength of the electromagnetic system of excitation of the resonator oscillations, $c(\varphi)$ is the rigidity of the elastic suspension of the ring resonator, which is set as follows:

$$c(\varphi) = C_m,\ \ \frac{\pi}{4}(m-1) < \varphi \le \frac{\pi}{4}(m-1) + \frac{h_T}{R},\ \ (m = 1, 2, ..., 8)\,, \tag{6}$$

where C_m is the stiffness coefficient of the m-th lamella of the elastic suspension, h_T is the nominal thickness of the lamella. Due to instrumental manufacturing errors, the rigidity and geometrical parameters of the elastic suspension may differ from the nominal values, but the splitting of the resonator oscillation frequencies caused by the indicated errors is significantly (by four orders of magnitude) less than the main natural oscillation frequency of the resonator.

To account for the non-uniform rigidity of the elastic suspension of the ring resonator, the Eq. (6) is represented as a Fourier series with respect to the circumferential angle φ:

$$c\left(\varphi\right) = c_0\left(1 + \sum_{k=1}^{N}\left(c_k \cos k\varphi + s_k \sin k\varphi\right)\right),\ \left(c_0 = \frac{h_T}{2\pi R}\sum_{k=1}^{8} C_k\right), \tag{7}$$

where $c_k, s_k\ \left(k = 1, 2, ..., N\right)$ are the dimensionless expansion coefficients characterizing the instrumental error in the manufacture of an elastic suspension. Note that in the design case of an equally rigid elastic suspension, the coefficients $c_k = s_k = 0\ \left(k = 1, 2, ..., 7\right)$.

To obtain the equations of motion of the resonator, the variational principle of Hamilton-Ostrogradsky [7], [9] is applied. For this purpose, the specific Lagrangian $L = T - P$ is formulated, by taking into account expressions (1), (5), and normalization, takes the following form (8):

$$L=\frac{1}{2}\left[\left(\dot{v}+\Omega\left(w+R\right)-V_1\sin\varphi+V_2\cos\varphi\right)^2+\left(\dot{w}-\Omega v+V_1\cos\varphi+V_2\sin\varphi\right)^2\right]- \\ -\frac{1}{2}\delta^2\left(v'+w\right)^2-\frac{1}{2}\kappa^2\left(v'-w''\right)^2-\frac{1}{2}\zeta\kappa^2\left(v^2+w^2\right), \tag{8}$$

parameters entered here:

$$\kappa^2=\frac{E\,I}{\rho SR^4(1+\mu_0)},\quad \zeta\kappa^2=\frac{c_0}{\rho SR(1+\mu_0)},\quad \delta^2=\frac{12R^2}{h^2}\kappa^2, \tag{9}$$

are characterizing the elastic properties of the system and having the dimension of the squared frequency.

In contrast to the established mathematical model describing the motion of a resonator with an inextensible median line [7], a more comprehensive model is constructed to represent the independent displacements of the elastic system denoted by v, w . An integral with fixed limits is introduced:

$$H=\int_{\varphi_1}^{\varphi_2}\int_{t_1}^{t_2}L\left(v,w,\dot{v},\dot{w},v',w',w''\right)dt\,d\varphi,$$

called the Hamiltonian action. In accordance with the variational Hamilton-Ostrogradsky principle, the first variation of the Hamiltonian action δH on the direct path of the system is equal to zero:

$$\delta H=0.$$

Variation of the action according to Hamilton yields the following result:

$$\delta H=\int_{\varphi_1}^{\varphi_2}\int_{t_1}^{t_2}\left(\frac{\partial L}{\partial v}\delta v+\frac{\partial L}{\partial w}\delta w+\frac{\partial L}{\partial\dot{v}}\delta\dot{v}+\frac{\partial L}{\partial\dot{w}}\delta\dot{w}+\right. \\ \left.+\frac{\partial L}{\partial v'}\delta v'+\frac{\partial L}{\partial w'}\delta w'+\frac{\partial L}{\partial w''}\delta w''\right)dt\,d\varphi=0. \tag{10}$$

Considering that the generalized coordinates of the system are elastic displacements v and w, whose variations δv and δw are both independent and arbitrary, the equations of motion of an elastic system take the form:

$$\begin{cases}\dfrac{d}{dt}\dfrac{\partial L}{\partial\dot{v}}+\dfrac{d}{d\varphi}\dfrac{\partial L}{\partial v'}-\dfrac{\partial L}{\partial v}=Q_v^*, \\ \dfrac{d}{dt}\dfrac{\partial L}{\partial\dot{w}}-\dfrac{d^2}{d\varphi^2}\dfrac{\partial L}{\partial w''}+\dfrac{d}{d\varphi}\dfrac{\partial L}{\partial w'}-\dfrac{\partial L}{\partial w}=Q_w^*,\end{cases} \tag{11}$$

where Q_v^*, Q_w^* are the dissipative forces:

$$Q_v^* = -\frac{\partial \Phi}{\partial \dot{v}},\ Q_w^* = -\frac{\partial \Phi}{\partial \dot{w}}.$$

The resulting equations are called the Lagrange equations for systems with distributed parameters.

2.2. Dynamics of a balanced resonator on a moving base

The design case of an equally rigid elastic suspension of a ring resonator is considered next. By applying the variational principle of Hamilton-Ostrogradsky, the equations of motion of the ring are obtained, accounting for dissipative forces:

$$\begin{cases} \ddot{v} + 2\Omega\dot{w} - \left(\dot{V}_1 - \Omega V_2\right)\sin\varphi + \left(\dot{V}_2 + \Omega V_1\right)\cos\varphi - \\ \quad -\delta^2\left(v'' - w'\right) + \kappa^2\left(w^{III} - v'' + \zeta v\right) + e_*\kappa^2\left(\dot{w}^{III} - \dot{v}''\right) = 0, \\ \ddot{w} - 2\Omega\dot{v} + \left(\dot{V}_2 + \Omega V_1\right)\sin\varphi + \left(\dot{V}_1 - \Omega V_2\right)\cos\varphi - \\ \quad -\delta^2\left(v' - w\right) + \kappa^2\left(w^{IV} - v^{III} + \zeta w\right) + e_*\kappa^2\left(\dot{w}^{IV} - \dot{v}^{III}\right) = 0, \end{cases} \tag{12}$$

where e_*, ζ_* are the damping coefficients:

$$e_* = \frac{E_*}{E},\ \ \frac{c_*}{\rho SR(1+\mu_0)} = \zeta_* e_* \kappa^2. \tag{13}$$

The Eqs. (12) omit small terms proportional to the angular acceleration $\dot{\Omega}$ and the square of the base angular velocity Ω^2. The solution of the Eqs. (12) in the multi-mode approximation using the Bubnov-Galerkin method for the elastic displacement function in the form:

$$\begin{cases} v = \sum_{k=1}^{N}\left(r_k(t)\cos k\varphi + s_k(t)\sin k\varphi\right), \\ w = \sum_{k=1}^{N}\left(f_k(t)\cos k\varphi + g_k(t)\sin k\varphi\right), \end{cases} \tag{14}$$

here r_k, s_k, f_k, g_k are the desired functions of time, k is the number of the oscillation mode of the elastic system, N is the number of modes.

As a result of substituting functions (14) into the Eqs. (12) and equating the coefficients of $\cos k\varphi$ and $\sin k\varphi$ to zero, the Bubnov-Galerkin method yields a system of N ordinary differential equations, with $N \to \infty$ equivalent to the original Eqs. (12). In the calculated case, the system of ordinary differential equations consists of unrelated

subsystems with the state vector $\mathbf{x}_k = \left(f_k, g_k, r_k, s_k \right)^T$ describing the oscillations of the resonator in a mode with a given number k. The resonator oscillation equations are written in the first mode in vector-matrix form:

$$\ddot{\mathbf{x}}_1 + \left(2\Omega\mathbf{J} + \mathbf{D}_{*1}\right)\dot{\mathbf{x}}_1 + \mathbf{D}_1\,\mathbf{x}_1 = \mathbf{w}, \tag{15}$$

where $\mathbf{D}_1$ is the matrix of positional forces; $\mathbf{D}_{*1}$ is the matrix of dissipative forces, which coincides in structure with $\mathbf{D}_1$ in accordance with the Kelvin-Voigt method; $\mathbf{J}$ is the block skew-symmetric matrix of gyroscopic forces; $\mathbf{w}$ is the vector of disturbing external influences:

$$\mathbf{D}_1 = \begin{pmatrix} \delta^2 + (\zeta+1)\kappa^2 & 0 & 0 & \delta^2 + \kappa^2 \\ 0 & \delta^2 + (\zeta+1)\kappa^2 & -\delta^2 - \kappa^2 & 0 \\ 0 & -\delta^2 - \kappa^2 & \delta^2 + (\zeta+1)\kappa^2 & 0 \\ \delta^2 + \kappa^2 & 0 & 0 & \delta^2 + (\zeta+1)\kappa^2 \end{pmatrix},$$

$$\mathbf{J} = \begin{pmatrix} 0 & 0 & -1 & 0 \\ 0 & 0 & 0 & -1 \\ 1 & 0 & 0 & 0 \\ 0 & 1 & 0 & 0 \end{pmatrix}, \tag{16}$$

$$\mathbf{w} = \left(-\dot{V}_1 + \Omega V_2, -\dot{V}_2 - \Omega V_1, -\dot{V}_2 - \Omega V_1, \dot{V}_1 - \Omega V_2\right)^T.$$

Note that the dynamics of the resonator in the first mode of oscillation is affected by the absolute linear acceleration of the base of the gyroscope $\dot{V}_1 - \Omega V_2$, $\dot{V}_2 + \Omega V_1$.

The vibration frequencies of a conservative elastic system can be determined from the first mode of vibration on a fixed base from the frequency equation:

$$\left(\zeta\kappa^2 - \omega^2\right)^2 \left(h^2\left((\zeta+2)\kappa^2 - \omega^2\right) + 24\kappa^2 R^2\right)^2 = 0,$$

whose roots are the squares of the natural frequencies of the elastic system have the form:

$$\omega_1^2 = \zeta\kappa^2, \quad \omega_2^2 = \left(\zeta+2\right)\kappa^2 + 2\delta^2.$$

Considering that the resonator thickness h is much smaller than the radius of the ring resonator R, strongly separated characteristic values of the frequency squares are obtained, since $\delta^2 = \kappa^2(12R^2/h^2)$. The lowest oscillation frequencies can be determined experimentally by constructing the amplitude-frequency characteristics of a prototype RMMG.

Differential equations describing free vibrations of a conservative system on a movable vibrating foundation in vibration modes with the number *k* look like (Fig. 2):

$$\begin{cases} \ddot{f}_k - 2\Omega\dot{r}_k + k\left(\delta^2 + \kappa^2 k^2\right)s_k + \left(\delta^2 + \kappa^2\left(\zeta + k^4\right)\right)f_k = 0, \\ \ddot{g}_k - 2\Omega\dot{s}_k - k\left(\delta^2 + \kappa^2 k^2\right)r_k + \left(\delta^2 + \kappa^2\left(\zeta + k^4\right)\right)g_k = 0, \\ \ddot{r}_k + 2\Omega\dot{f}_k - k\left(\delta^2 + \kappa^2 k^2\right)g_k + \left(\delta^2 k^2 + \kappa^2\left(\zeta + k^2\right)\right)r_k = 0, \\ \ddot{s}_k + 2\Omega\dot{g}_k + k\left(\delta^2 + \kappa^2 k^2\right)f_k + \left(\delta^2 k^2 + \kappa^2\left(\zeta + k^2\right)\right)s_k = 0, \ \left(k = 2,3,...\right). \end{cases} \tag{17}$$

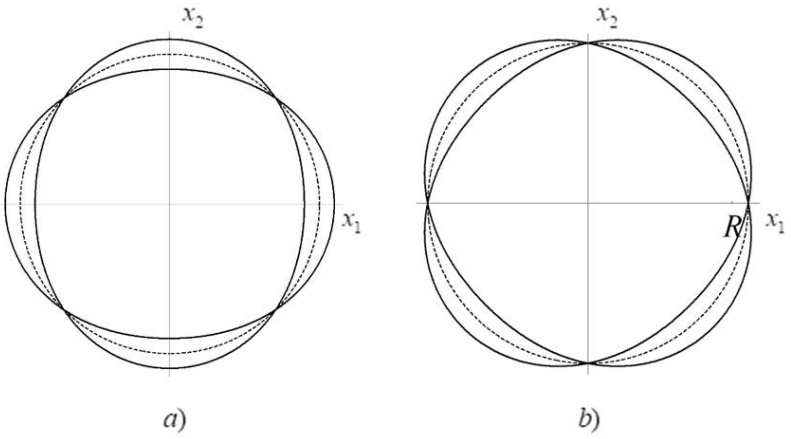

Fig. 2. First (a) and second (b) mode shapes of elastic oscillations of the ring resonator.

For the subsequent analysis of the dynamics of an unbalanced resonator, the resonator oscillation Eqs. (17) are written in vector-matrix form, taking into account dissipative forces:

$$\ddot{\mathbf{x}}_k + \left(2\Omega\mathbf{J} + \mathbf{D}_{*k}\right)\dot{\mathbf{x}}_k + \mathbf{D}_k\,\mathbf{x}_k = 0, \quad \left(k = 2,3,...\right), \tag{18}$$

$$\mathbf{D}_k = \begin{pmatrix} \delta^2 + (\zeta + k^4)\kappa^2 & 0 & 0 & k\left(\delta^2 + \kappa^2 k^2\right) \\ 0 & \delta^2 + (\zeta + k^4)\kappa^2 & -k\left(\delta^2 + \kappa^2 k^2\right) & 0 \\ 0 & -k\left(\delta^2 + \kappa^2 k^2\right) & \delta^2 + (\zeta + k^4)\kappa^2 & 0 \\ k\left(\delta^2 + \kappa^2 k^2\right) & 0 & 0 & \delta^2 + (\zeta + k^4)\kappa^2 \end{pmatrix}.$$

Note that the damping coefficients $\mathbf{D}_{*k}$ can be determined experimentally. An analysis of the Eqs. (17) shows that shocks and vibrations of the base do not affect the dynamics of a balanced resonator in the second main form of oscillation [7].

3. Effect of vibrations

3.1. Influence of impact actions on the mechanical design of a balanced gyroscope

Within the time interval of the maximum shock acceleration, the losses due to vibrations of the elastic system can be neglected. An analysis of the initial data on external

influencing factors shows that when the gyroscope is exposed to vibroshocks, the frequency content of external vibrations is significantly lower than the lowest natural frequency of bending vibrations of the elastic system, so that the process of loading the elastic system can be considered as quasi-static [7].

To calculate the maximum deformations of the structure, a particular solution of the Eqs. (17) is written out:

$$\bar{\mathbf{x}}_1 = \mathbf{D}^{-1}\mathbf{w},$$

$$\bar{f}_1 = -\frac{\dot{V}_1}{\zeta\kappa^2}, \quad \bar{g}_1 = -\frac{\dot{V}_2}{\zeta\kappa^2}, \quad \bar{r}_1 = -\frac{\dot{V}_2}{\zeta\kappa^2}, \quad \bar{s}_1 = \frac{\dot{V}_1}{\zeta\kappa^2}.$$

An analysis of the obtained particular solution of the Eqs. (17) shows that the maximum deformation of the resonator is proportional to the magnitude of the peak impact acceleration and inversely proportional to the square of the lowest natural frequency in the first natural mode of oscillation.

Numeric example: A numerical estimation is performed for the parameters of the ring resonator model (from [7]) with a radius of $R = 3$ mm, a rectangular cross section with a thickness $h = 120$ μm, a height $b = 100$ μm, with a resonator material density of $\rho = 2328$ kg/m^3 and Young's modulus $E = 168.9$ GPa. The calculated value of the lowest natural frequency of oscillations of the resonator according to the first form of oscillations $\omega_1^{(1)} = \sqrt{\zeta}\kappa$ will be taken equal to $\omega_1^{(1)} = 14$ kHz. For a peak impact acceleration of $\dot{V}_2 = 800$ m/s^2 directed in the plane of the ring resonator along the axis x_2, the following holds:

$$\bar{g}_1 = \bar{r}_1 = -\frac{\dot{V}_2}{\zeta\kappa^2} = -\frac{800}{2\pi 14000^{\,2}} = -0.1 \text{ μm}, \quad \bar{f}_1 = \bar{s}_1 = 0.$$

In accordance with the single-mode representation Eqs. (14) the maximum displacement of the elastic system will occur in the first form:

$$v = \bar{r}_1 \cos\varphi, \; w = \bar{g}_1 \sin\varphi.$$

By differentiating the obtained functions in accordance with Eq. (4), an expression for the circumferential deformation of the ring is obtained: $e = 0$, given that $v' + w = 0, \; v' - w'' = 0$.

An analysis of the results obtained shows that when the ring resonator moves along the first form, the ring as a whole is displaced, while additional stresses do not arise in the ring cross section. The main load is distributed on the elastic suspension, the

maximum displacement of which is $\bar{g}_1 = \bar{r}_1 = -0.1$ μm, comparable to the nominal values of the structure deformations in the design shock-free operation mode. With uniaxial tensile-compressive strain, the maximum value of the stress in the lamella cross section is $\sigma = E\,e = 16.89$ kPam, which is significantly less than the limit values.

3.2. Influence of random vibrations of the base on the mechanical design of a balanced gyroscope

Next, the effect of random vibrations of the RMMG base on the dynamics of the elastic system is considered in terms of the first form of vibrations. The equations of motion of the system Eqs. (15) are written in the first form in the Cauchy form:

$$\dot{\mathbf{y}} = \mathbf{A}\mathbf{y} + \mathbf{w}, \tag{19}$$

where $\mathbf{y} = \left[f_1, g_1, r_1, s_1, \dot{f}_1, \dot{g}_1, \dot{r}_1, \dot{s}_1 \right]^T$ is the system state vector, $\mathbf{w}$ is the vector of random actions on the system, $\mathbf{A}$ is the matrix of the system.

The system is assumed to be affected by a stationary random process of the white noise type with zero mathematical expectation $M\ \mathbf{w}(t) = 0$, a given intensity G, and a correlation function:

$$M\left[\mathbf{w}(t)\mathbf{w}^T(\tau)\right] = \mathbf{G}\,\delta(t-\tau), \tag{20}$$

where $\delta(t-\tau)$ is the delta function.

The mathematical expectations of the output variables $M[\mathbf{y}] = \mathbf{m}_y$ of the system under consideration can be obtained if, in the system of differential equations, Eq. (19) the input signals and the initial conditions of the state vector are replaced by their mathematical expectations $M[\mathbf{y}_0] = \mathbf{m}_{y_0}$.

Integration of the system of differential equations for the mathematical expectations of the output variables $\dot{\mathbf{m}}_y = \mathbf{A}\mathbf{m}_y$ presents no practical difficulties. Given that there are signals with zero mathematical expectation at the input of the system, the steady-state values of the variables $\mathbf{m}_y$ are equal to zero.

To determine the dispersions and correlation moments of the output signals of the system, the matrix is introduced:

$$M\left[\mathbf{y}(t)\mathbf{y}^T(t)\right] = \mathbf{R}_y(t), \tag{21}$$

and the differential equation is written:

$$\dot{\mathbf{R}}_y = \mathbf{A}\mathbf{R}_y + \mathbf{R}_y\mathbf{A}^T + \mathbf{G}, \tag{22}$$

obtained by differentiation Eq. (21) due to the Eqs. (19) and properties of the solution of the differential equation and the delta function [33]-[34]. The diagonal elements of $\mathbf{R}_y(t)$ the differential equation solution matrix (22) give the values of the variances of the output signals of the system, and the off-diagonal elements determine the corresponding correlation moments.

Given the symmetry of the system and the dimension of the original differential equations equal to eight, it is required to solve a system of differential equations of order 36 (8 equations for determining dispersions and 28 equations for correlation moments).

Note that the above method is also suitable in the case when the input signals of the system are not white noise, but can be represented as a white noise transformation by a shaping filter described by a finite-order differential equation. In this case, the equations of the shaping filter are added to the differential equations describing the original system.

For a stationary random function with zero mathematical expectation, spectral density $s_w(\omega)$ and correlation function $r_w(\tau)$:

$$s_w(\omega) = \frac{D}{\pi}\,\frac{\alpha}{\alpha^2+\omega^2},\quad r_w(\tau) = De^{-\alpha|\tau|},$$

the shaping filter is an aperiodic link with a transfer function $\Phi(p) = \dfrac{K}{Tp+1}$ with a time constant $T = 1/\alpha$ and gain $K = \sqrt{2D/\alpha}$.

In this case, the spectral density can be represented as:

$$s_w(\omega) = \frac{1}{2\pi}\left|\Phi(i\omega)\right|^2.$$

The aperiodic link has the property of a filter and significantly reduces the amplitude of harmonic effects with frequencies greater than the cutoff frequency $1/T = \alpha$.

In the case of a stationary random signal at the system input, the moments of the system output signals in the steady state are determined by a particular solution of the Eqs. (22), i.e. solution of the algebraic matrix equation:

$$\mathbf{A}\mathbf{R}_y + \mathbf{R}_y\mathbf{A}^T + \mathbf{G} = 0. \tag{23}$$

Next, consider an example of calculating the elastic displacements of an oscillatory system under the influence of random vibrations of the base in the plane of the ring resonator.

Numeric example: Taking into account the significantly different motion scales of the initial elastic system and the numerical estimates of the oscillation frequencies in the first mode along with the damping coefficient γ of the oscillatory circuit, the system equations describing the low-frequency oscillations in the first mode and the shaping filter equation are formulated as follows:

$$\begin{aligned} &\ddot{f} + \gamma \dot{f} + \omega_1^2 f = W, \\ &T\dot{W} + W = KV. \end{aligned} \tag{24}$$

The input action of the shaping filter is a stationary random process V of the type of white noise of unit intensity. The output signal of the shaping filter and the input action on the oscillatory system is the absolute acceleration of the base W in the form of a stationary random process with a given spectral density.

In accordance with Eqs. (24), the state vector $\mathbf{y} = f, \dot{f}, W^T$ is introduced, and the matrices of system Eqs. (22) are expressed as follows:

$$\mathbf{A} = \begin{pmatrix} 0 & 1 & 0 \\ -\omega_1^2 & -\gamma & 1 \\ 0 & 0 & -1/T \end{pmatrix}, \quad \mathbf{G} = \begin{pmatrix} 0 & 0 & 0 \\ 0 & 0 & 0 \\ 0 & 0 & K^2/T^2 \end{pmatrix}, \quad \mathbf{R}_y = \begin{pmatrix} r_{11} & r_{12} & r_{13} \\ r_{12} & r_{22} & r_{23} \\ r_{13} & r_{23} & r_{33} \end{pmatrix},$$

where r_{11} is the dispersion of the output vibration displacement of the elastic oscillatory system; r_{22} is the dispersion of the output linear velocity of the vibration displacement of the system; r_{33} is the dispersion of vibration acceleration of the base; the off-diagonal elements of the symmetric matrix R_y are the correlation moments of the components of the state vector and the shaping filter.

The solution of the dispersion Eq. (23) has the form:

$$r_{11} = \frac{D(\alpha+\gamma)}{\gamma\omega_1^2\left(\alpha(\alpha+\gamma)+\omega_1^2\right)}, \quad r_{12} = 0, \quad r_{13} = \frac{D}{\alpha(\alpha+\gamma)+\omega_1^2},$$

$$r_{22} = \frac{\alpha D}{\gamma\left(\alpha(\alpha+\gamma)+\omega_1^2\right)}, \quad r_{23} = \frac{\alpha D}{\alpha(\alpha+\gamma)+\omega_1^2}, \quad r_{33} = D.$$

An analysis of the obtained solution shows that the dispersion of the output vibration displacement $r_{11} = \sigma_f^2$ of the elastic system is proportional to the dispersion of the vibration acceleration of the base $D = \sigma_w^2$ and depends nonlinearly on the damping

coefficient γ, the cutoff frequency of the shaping filter α and the natural frequency of the first mode of vibration ω_1.

At the cutoff frequency of the shaping filter, defined as $\alpha = \omega_1 / 3$, and the damping coefficient $\gamma = \omega_1 / Q$ where Q is the quality factor of the oscillatory circuit, the dispersion of the output vibration displacement of the elastic system is given by: $r_{11} = \frac{3DQ}{10\omega_1^4}$.

Thus, the standard deviation for broadband random vibration can be estimated by the formula: $\sigma_f = \sqrt{\frac{3Q}{10}} \frac{\sigma_w}{\omega_1^2}$.

For a quality factor $Q = 2000$, an oscillation frequency in the first form $\omega_1 = 14$ kHz, and a standard deviation of external vibration $\sigma_w = 40$ m/s^2 with zero mathematical expectation, the resulting standard deviation is $\sigma_f = 0.1$ μm.

Analysis of the obtained results shows that multiple vibroshocks, broadband vibration in the frequency range up to 4 kHz does not affect the mechanical strength of the structure. Thus, the stresses arising in the mechanical structure under shock and vibration effects do not exceed the permissible limit values.

4. Conclusions

The study has developed a mathematical model describing the motion of the MEMS gyroscope sensing element in the form of a thin elastic ring within an elastic suspension system. Based on this model, the vibration of the elastic system under shock and vibration excitation was simulated using the multi-order approximation method. The model determines the elastic deformations and stresses arising in the mechanical structure mounted on a movable base when subjected to external dynamic loading. The analysis reveals that the primary destructive impact of base-induced shocks and vibrations is concentrated in the first mode of resonator oscillations. In this mode, the maximum deformation of the resonator under quasi-stationary loading conditions is shown to be directly proportional to the peak impact acceleration and inversely proportional to the square of the fundamental natural frequency. During oscillations in the first mode, the entire ring undergoes displacement, resulting in the elastic suspension bearing the majority of the load, with its maximum displacement remaining within the nominal deformation range specified for shock-free operation. Under uniaxial tensile-compressive stress conditions, the peak stress in the elastic suspension does not exceed permissible limits. Moreover, the dynamics of the balanced resonator in the second principal vibration mode are largely unaffected by shocks and vibrations, consistent with the baseline

operational mode of the RMMG. However, manufacturing imperfections can disturb resonator symmetry, introducing coupling between vibration modes. In the second vibration mode, shocks and vibrations influence only the accuracy of wave pattern measurements, without significantly altering system dynamics. The results confirm the adequacy of the developed mathematical model for analyzing the dynamic behavior of micromechanical ring resonators under external mechanical disturbances. Future research will focus on refining the model by incorporating material properties. Experimental validation of the theoretical findings under controlled shock and vibration conditions will also be pursued to enhance the model's applicability in practical RMMG design.

Acknowledgement

The author would like to thank Prof. Igor V. Merkuryev at National Research University "Moscow Power Engineering Institute", Moscow, Russian Federation for his help. This research is funded by Le Quy Don Technical University Research Fund under the grant number 24.1.32.

References

[1] B. A. Kozlov and I. A. Ushakov, *Handbook for Calculating the Reliability of Radio Electronics and Automation Equipment*. Moscow: Soviet Radio, 472p, 1975 (English Translation).

[2] I. A. Ushakova, *Reliability of Technical Systems Handbook*. Moscow: Radio and Communication, 608p, 1985 (English Translation).

[3] M. A. Basarab, V. F. Kravchenko, and V. A. Matveev, *Mathematical Modeling of Physical Processes in Gyroscopy*. Moscow: Radio Engineering, 176p, 2005 (English Translation).

[4] V. F. Zhuravlev and D. M. Klimov, *Wave Solid-state Gyroscope*, Moscow: Nauka, 125p, 1985 (English Translation).

[5] V. F. Zhuravlev, "Drift of an imperfect WTG", *Izv. RAN. MTT*., No. 4, pp. 19-23, 2004, *Mechanics of Solids* (English Translation).

[6] E. P. Kubyshkin and N. B. Fedotov, "Peculiarities of the effect of vibration on the behavior of the wave pattern of a ring resonator", *Izv. RAN. MTT*., No. 5, pp. 42-47, 1995, *Mechanics of Solids* (English Translation).

[7] I. V. Merkuriev and V. V. Podalkov, *Dynamics of Micromechanical and Wave Solid-state Gyroscopes*, M. Fizmatlit, 228p, 2009 (English Translation).

[8] M. N. Kirsanov, "Bending torsion and asymptotic analysis of the spatial rod console", *Inzhenernostroitelnyi Zhurnal*, No. 5, pp. 37-43, 2014 (English Translation).

[9] M. N. Kirsanov, *Maple and Maplet. Solutions of Problems of Mechanics*, Saint Petersburg: Lan, 512p, 2012 (English Translation).

[10] F. Ayazi and K. Najafi, "A HARPSS polysilicon vibrating ring gyroscope", *Journal of Microelectromechanical Systems*, No. 10, pp. 169-179, 2001. DOI: 10.1109/84.925732

[11] Y. G. Martynenko, I. V. Merkuriev, and V. V. Podalkov, "Dynamics of a ring micromechanical gyroscope in the forced-oscillation mode", *Gyroscopy and Navigation*, No. 1, pp. 43-51, 2010. DOI: 10.1134/s2075108710010074

[12] S.W. Yoon, S. Lee, and K. Najafi, "Vibration sensitivity analysis of MEMS vibratory ring gyroscopes", *Sensors and Actuators*, No. 171, pp. 163-177, 2011. DOI: 10.1016/j.sna.2011.08.010

[13] A. A. Maslov, I. V. Merkuryev, and V. V. Podalkov, "External vibration and shock impact on the dynamics of micromechanical gyroscopes", *22nd Saint Petersburg International Conference on Integrated Navigation Systems*, Saint Petersburg, pp. 327-328, 2015.

[14] D. A. Maslov and I. V. Merkuryev, "Impact of nonlinear properties of electrostatic control sensors on the dynamics of a cylindrical resonator of a wave solid-state gyroscope", *Mechanics of Solids*, Vol. 56, No. 6, pp. 960-979, 2021. DOI: 10.3103/S002565442106011X

[15] A. A. Maslov, D. A. Maslov, I. V. Merkuryev, and V. V. Podalkov, "Methods to eliminate nonlinearity of electrostatic control sensors of the wave solid-state gyroscope", *Anniversary 25th International Conference on Integrated Navigation Systems*, Saint Petersburg, 2018. DOI: 10.23919/ICINS.2018.8405895

[16] A. A. Maslov, D. A. Maslov, and I. V. Merkuryev, "The effect of the reference voltage on the drift of a wave solid-state gyroscope with flat electrodes", *Anniversary 30th International Conference on Integrated Navigation Systems*, Saint Petersburg, 2023. DOI: 10.23919/ICINS51816.2023.10168316

[17] A. A. Maslov, D. A. Maslov, and I. V. Merkuryev, "Nonlinear effects in the dynamics of HRG with flat electrodes", *Gyroscopy and Navigation*, No. 14, pp. 320-327, 2024. DOI: 10.1134/S2075108724700044

[18] S. Yu *et al.*, "Real-time correction of gain nonlinearity in electrostatic actuation for whole-angle micro-shell resonator gyroscope", *Microsystems & Nanoengineering*, No. 10, 2024. DOI: 10.1038/s41378-024-00818-x

[19] J. Sun *et al.*, "Investigation of angle drift induced by actuation electrode errors for whole-angle micro-shell resonator gyroscope", *IEEE Sensors Journal*, Vol. 22, No. 4, pp. 3105-3112, 2022. DOI: 10.1109/JSEN.2022.3140799

[20] Z. Wei, G. Yi, Y. Huo, Z. Qi, and Z. Xu, "The synthesis model of flat-electrode hemispherical resonator gyro", *Sensors*, No. 19, Iss.7, 2019. DOI: 10.3390/s19071690

[21] Y. Li, Q. Tan, J. Wen, L. Song, and F. Yang, "Study of nonlinear vibration of resonant gyroscope based on uncertainty analysis method", *Microelectronic Engineering*, Vol. 263, 2022. DOI: 10.1016/j.mee.2022.111845

[22] S. Hao *et al.*, "Critical parameters and influence on dynamic behaviours of nonlinear electrostatic force in a micromechanical vibrating gyroscope", *Shock Vibration*, Vol. 12, pp. 1-15, 2020. DOI: 10.1155/2020/8880124

[23] S. Yang, W. Feng, S. Wang, and J. Li, "A SINS/CNS integrated navigation scheme with improved mathematical horizon reference", *Measurement*, Vol. 195, 2022. DOI: 10.1016/j.measurement.2022.111028

[24] T. S. Amer, R. Starosta, A. Almahalawy, and A. S. Elameer, "The stability analysis of a vibrating auto-parametric dynamical system near resonance", *Applied Sciences*, Vol. 12, No. 3, pp. 1-35, 2022. DOI: 10.3390/app12031737

[25] M. A. Bek, T. S. Amer, A. Almahalawy, and A. S. Elameer, "The asymptotic analysis for the motion of 3DOF dynamical system close to resonances", *Alexandria Engineering Journal*, Vol. 60, Iss. 4, pp. 3539-3551, 2021. DOI: 10.1016/j.aej.2021.02.017

[26] T. S. Amer, "On the rotational motion of a gyrostat about a fixed point with mass distribution", *Nonlinear Dynamics*, Vol. 54, pp. 189-198, 2008. DOI: 10.1007/s11071-007-9320-4

[27] T. S. Amer, H. F. El-Kafly, A. H. Elneklawy, and A. A. Galal, "Stability analysis of a rotating rigid body: The role of external and gyroscopic torques with energy dissipation", *Journal of Low Frequency Noise, Vibration & Active Control*, Vol. 44, No. 3, pp. 1502-1515, 2025. DOI: 10.1177/14613484251324586

[28] T. S. Amer, A. H. Elneklawy, and H. F. El-Kafly, "Dynamical motion of a spacecraft containing a slug and influenced by a gyrostatic moment and constant torques", *Journal of Low Frequency Noise, Vibration & Active Control*, Vol. 44, No. 3, pp. 1708-1725, 2025. DOI: 10.1177/14613484251322235

[29] T. S. Amer, A. H. Elneklawy, and H. F. El-Kafly, "Analysis of Euler's equations for a symmetric rigid body subject to time-dependent gyrostatic torque", *Journal of Low Frequency Noise, Vibration & Active Control*, Vol. 44, No. 2, pp. 831-842, 2025. DOI: 10.1177/14613484241312465

[30] T. S. Amer, W. S. Amer, M. Fakharany, A. H. Elneklawy, and H. F. El-Kafly, "Modeling of the Euler-Poisson equations for rigid bodies in the context of the gyrostatic influences: An innovative methodology", *European Journal of Pure and Applied Mathematics*, Vol. 18, No. 1, pp. 1-14, 2025. DOI: 10.29020/nybg.ejpam.v18i1.5712

[31] N. N. Bogolyubov and Yu. A. Mitropolsky, *Asymptotic Methods in the Theory of Nonlinear Oscillations*. Moscow: Nauka, 1974, 503p (English Translation).

[32] A. V. Bulinsky and A. N. Shiryaev, *Theory of Random Processes*, Moscow: Fizmatlit, 2003, 400p (English Translation).

[33] K. A. Pupkov, E. M. Voronov, and Yu. P. Kornyushin, *Methods of Classical and Modern Theory of Automatic Control, V.2: Statistical Dynamics and Identification of Automatic Control Systems*. Moscow: Publishing House of MSTU im. N. E. Bauman, 2004, 640p (English Translation).

[34] V. A. Afanasiev, N. Yu. Afanasiev, and V. S. Kazakov, *Theory of Automatic Control. Continuous and Impulse Systems, Statistical Dynamics of Linear Systems*. Izhevsk: Publishing House of IzhGTU, 2007, 388p (English Translation).

[35] I. Yu. Sirotin and M. P. Shaskolskaya, *Fundamentals of Crystal Physics*. Moscow: Nauka, 1975, 680p (English Translation).

ẢNH HƯỞNG CỦA RUNG CHẤN ĐẾN ĐỘNG LỰC HỌC CON QUAY HỒI CHUYỂN VI CƠ DẠNG VÒNG NHẪN

Vũ Thế Trung Giáp[1]

[1]*Khoa Hàng không Vũ trụ, Trường Đại học Kỹ thuật Lê Quý Đôn*

Tóm tắt: Bài báo trình bày về động lực học của con quay hồi chuyển vi cơ với bộ cộng hưởng vòng nhẫn (RMMG), được sử dụng trong các hệ thống định vị và điều khiển chuyển động. Phần tử cảm ứng của RMMG là một vòng nhẫn mỏng đàn hồi được giữ bởi một hệ thống treo đàn hồi, giúp phát hiện các dao động uốn nhỏ để đo chuyển động góc. Nghiên cứu phân tích ảnh hưởng của rung sốc bên ngoài đến thiết kế cơ học của bộ cộng hưởng vòng nhẫn. Một mô hình toán học được xây dựng dựa trên nguyên lý biến phân Hamilton-Ostrogradsky và phương pháp chiếu Bubnov-Galerkin để phân tích các dao động của cơ hệ. Kết quả cho thấy rung sốc chủ yếu ảnh hưởng đến chế độ dao động thứ nhất, với độ biến dạng cực đại của bộ cộng hưởng tỉ lệ thuận với độ lớn của gia tốc va chạm cực đại và tỉ lệ nghịch với bình phương tần số riêng thấp nhất trong chế độ dao động riêng thứ nhất. Dạng dao động cơ bản thứ hai của bộ cộng hưởng vòng nhẫn không bị ảnh hưởng trong điều kiện bình thường. Ngoài ra, các sai số gia công có thể gây ra sự mất đối xứng, làm ảnh hưởng đến độ chính xác của phép đo. Kết quả của nghiên cứu này cung cấp những hiểu biết góp phần cải thiện mô hình thiết kế nhằm nâng cao độ chính xác của RMMG khi chịu tác động của các rung chấn bên ngoài.

Từ khóa: *Con quay vi cơ; bộ cộng hưởng vòng nhẫn; phi tuyến.*

Received: 23/09/2025; Revised: 02/12/2025; Accepted for publication: 27/01/2026

❑